

Combining Gradients and Probabilities for Heterogeneous Approximation of Neural Networks

Elias Trommer
elias.trommer@infineon.com
Infineon Technologies
Dresden, Germany

Bernd Waschneck
bernd.waschneck@infineon.com
Infineon Technologies
Dresden, Germany

Akash Kumar
akash.kumar@tu-dresden.de
Center for Advancing Electronics
Dresden (cfaed)
Dresden, Germany

ABSTRACT

This work explores the search for heterogeneous approximate multiplier configurations for neural networks that produce high accuracy and low energy consumption. We discuss the validity of additive Gaussian noise added to accurate neural network computations as a surrogate model for behavioral simulation of approximate multipliers. The continuous and differentiable properties of the solution space spanned by the additive Gaussian noise model are used as a heuristic that generates meaningful estimates of layer robustness without the need for combinatorial optimization techniques. Instead, the amount of noise injected into the accurate computations is learned during network training using backpropagation. A probabilistic model of the multiplier error is presented to bridge the gap between the domains; the model estimates the standard deviation of the approximate multiplier error, connecting solutions in the additive Gaussian noise space to actual hardware instances. Our experiments show that the combination of heterogeneous approximation and neural network retraining reduces the energy consumption for multiplications by 70% to 79% for different ResNet variants on the CIFAR-10 dataset with a Top-1 accuracy loss below one percentage point. For the more complex Tiny ImageNet task, our VGG16 model achieves a 53% reduction in energy consumption with a drop in Top-5 accuracy of 0.5 percentage points. We further demonstrate that our error model can predict the parameters of an approximate multiplier in the context of the commonly used additive Gaussian noise (AGN) model with high accuracy. Our software implementation is available under <https://github.com/etrommer/agn-approx>.

KEYWORDS

neural networks, approximate computing, energy efficiency

ACM Reference Format:

Elias Trommer, Bernd Waschneck, and Akash Kumar. 2022. Combining Gradients and Probabilities for Heterogeneous Approximation of Neural Networks. In *IEEE/ACM International Conference on Computer-Aided Design (ICCAD '22)*, October 30–November 3, 2022, San Diego, CA, USA. ACM, New York, NY, USA, 9 pages. <https://doi.org/10.1145/3508352.3549329>

Permission to make digital or hard copies of all or part of this work for personal or classroom use is granted without fee provided that copies are not made or distributed for profit or commercial advantage and that copies bear this notice and the full citation on the first page. Copyrights for components of this work owned by others than the author(s) must be honored. Abstracting with credit is permitted. To copy otherwise, or republish, to post on servers or to redistribute to lists, requires prior specific permission and/or a fee. Request permissions from permissions@acm.org.

ICCAD '22, October 30–November 3, 2022, San Diego, CA, USA

© 2022 Copyright held by the owner/author(s). Publication rights licensed to ACM.

ACM ISBN 978-1-4503-9217-4/22/10...\$15.00

<https://doi.org/10.1145/3508352.3549329>

1 INTRODUCTION

The power consumption of neural networks (NNs) has long been a major obstacle for their deployment inside power-constrained edge devices [37]. Particularly their computational complexity is a concern. Approximate arithmetic units have been proposed by the research community to address these issues [20, 24, 40]: relaxing the constraints imposed on the accuracy of operations enables new optimizations of arithmetic hardware, allowing for improved latency, energy consumption and area usage. Because of the dominant impact of multiplications, most efforts have been focused on improving the performance of multipliers using approximation—a rationale that this work builds upon as well.

Recent findings in the field of quantization demonstrate that optimizing quantization bit widths individually for each layer can provide higher accuracy compared to solutions that uniformly quantize the entire network. While some of these approaches rely on reinforcement learning [7, 36], an alternative route is the optimization of quantization parameters using gradient-based methods during network training [19, 38, 39]. To the best of our knowledge, the only work that investigates a non-uniform (i.e. heterogeneous) approach to approximation of NNs is Mrazek et al. [25], which uses a multi-objective genetic algorithm. By relying on behavioral simulation to evaluate a large number of candidate solutions, this method can not perform retraining, as it would render the already lengthy search procedure computationally intractable. Recent work by De la Parra et al. [3] demonstrates that solutions employing a single approximate multiplier (AM) throughout the entire network can outperform heterogeneous solutions if lost accuracy is recovered using retraining. Naturally, this raises the question whether performance could be improved even further if heterogeneous approximation and retraining were combined. It is obvious that this requires a different approach to finding a heterogeneous multiplier configuration in order for the search procedure to be feasible. To address this problem, we propose a gradient-based search algorithm that is capable of finding high-quality heterogeneous AM configurations. The search results in only a single candidate solution (or a small set acquired by varying a hyperparameter) that can easily be retrained. The key novel contributions of this work are:

- An efficient method for jointly determining the robustness to approximate multiplications for each NN layer during training. Through transformation into a more favorable solution space, our algorithm allows for a fast traversal of the heterogeneous multiplier assignment problem in a NN.

- A probabilistic error model that can give a precise estimate of the performance of an AM in a NN layer in terms of recoverable and non-recoverable error. Besides knowledge of the difference between the accurate and approximate multiplication results for all operand combinations, no behavioral simulation is required. The model is data-driven and does not assume any particular distribution of input operands. This makes its performance agnostic to methods that impact these distributions such as pruning [10, 33], quantization [41], etc.

Our evaluation of several convolutional neural network (CNN) models on the CIFAR-10 and Tiny ImageNet datasets shows that our method consistently manages to push the boundary of energy efficiency and network performance for various networks. We also improve upon existing models that express AM properties as additive Gaussian noise (AGN) parameters. This boosts the accuracy of AGN as a faster and simpler replacement for behavioral simulation of AMs.

2 BACKGROUND AND RELATED WORK

Due to the significant complexity of accurately simulating AMs during the training procedure of NNs [4, 35], several works propose the use of random noise as a replacement for the inaccurate computations. Hammad et al. [9] use a model based on the multiplier's Mean Relative Error (MRE) to generate random data which perturbs the output of an accurate computation. To enable retraining without the need for hardware simulation, De la Parra et al. [5] propose a data-driven noise model with higher granularity. The model constructs a noise tensor individually for each neuron by observing the approximation error on sample data. Similar to behavioral simulation, this model is not generalizable across AM instances because it only captures the dynamics of the AM it was constructed for.

Noisy intermediate results have also been used to demonstrate that the robustness in a NN is not uniform but varies for different layers [2]. These findings are corroborated by Hanif et al. [11], who determine the individual robustness of layers to approximation by injecting AGN into individual layers and observing the change in accuracy. By optimizing one layer at a time, the work does not take into account interdependencies between the robustness of layers. It also lacks a method that connects the robustness of a given layer to a concrete hardware instance. A similar method in the context of Capsule Networks is discussed by Marchisio et al. [21]. The proposed model for connecting a layer's robustness to noise with AM instances requires Monte Carlo (MC) simulations to be carried out for each combination of layer and AM. Other models that describe the error incurred by a single approximate multiplication were put forward by Mazahir et al. [22] and Ullah et al. [34]. These models, however, do not consider the compounding effects of multiple operations in a neural network.

To leverage the varying robustness of layers Mrazek et al. [25] demonstrate the use of a multi-objective evolutionary algorithm as a means to tackle the large search space of heterogeneous multiplier assignment in a NN. This solution relies on the evaluation of numerous candidate solutions, requiring the use of a weight remapping scheme rather than retraining to recover the degraded accuracy. Even without retraining, the vast number of simulations makes the method prohibitively slow for non-trivial networks. The

same is true for more recent approaches that optimize the network architecture itself for use with AMs [27].

3 PROPOSED METHODOLOGY

We provide an analysis of the aggregate error at a neuron's output and conclude that AGN is a meaningful surrogate model for behavioral simulation of AMs. Using the properties of this model, we demonstrate how to simultaneously optimize the amount of AGN across the entire network, considering the complex interactions between perturbations in different layers. An error model is developed in order to make the abstract AGN parameter comparable with the computation errors exhibited by concrete AM instances. Using the learned robustness parameters and the error model, we can determine which AMs will produce the required accuracy and match appropriate AM instances based on each layer's individual sensitivity.

3.1 Modeling approximate multiplication as noise

The error imposed by a single approximate multiplication can be considered additive to the output of an accurate multiplication

$$\tilde{f}(x, w) = x \cdot w + e(x, w) \quad (1)$$

where $e(x, w)$ is an error function that is unique to each AM instance. For a NN application we are, however, not concerned with the error of each individual operation, but with the *aggregate* error over several multiplications. With the definition of the pre-activation output of an accurate neuron

$$y = \sum_{i=1}^n x_i w_i + b \quad (2)$$

Equation (1) can be substituted to obtain the output of the same neuron using approximate multiplication as:

$$\tilde{y} = \sum_{i=1}^n x_i w_i + e(x_i, w_i) + b \quad (3)$$

$$= \underbrace{\sum_{i=1}^n x_i w_i + b}_{\text{Accurate Neuron}} + \underbrace{\sum_{i=1}^n e(x_i, w_i)}_{\text{Aggregate Error}} \quad (4)$$

Assuming that x and w exhibit sufficiently random properties, we conjecture that, as n grows, the distribution of the aggregate error will converge to a normal distribution, thus:

$$\tilde{y} \approx \sum_{i=1}^n x_i w_i + b + \mathcal{N}(\mu_e, \sigma_e) \quad (5)$$

$$= \sum_{i=1}^n x_i w_i + b + \mu_e + \sqrt{\sigma_e} \cdot \mathcal{N}(0, 1) \quad (6)$$

Furthermore, the systematic portion of the error μ_e will be absorbed by the bias or subsequent batch normalization for any non-degenerate case when the network is retrained to match the approximate configuration [31] s.t. $b' = b - \mu_e$. To simulate the effect of approximation on a fully retrained network, we can therefore assume that $\mu_e = 0$.

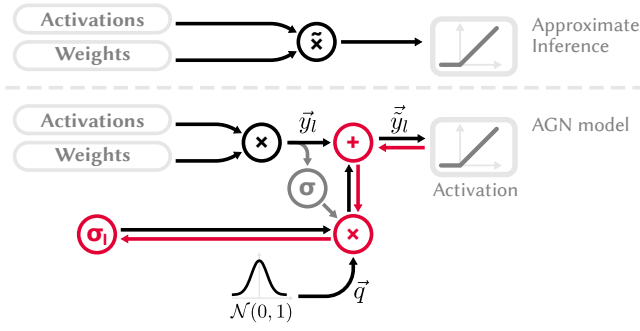


Figure 1: Substituting behavioral simulation of approximate multiplication with parameterized injection of AGN in a single layer (bias/batch normalization omitted for clarity). Highlighted operations mark backward pass of gradient for σ_l w.r.t. task loss.

Using this surrogate model instead of a behavioral simulation of the approximation error has two important benefits for the search procedure: First, AGN can easily be constructed using primitives that are available in most common deep learning toolkits and does not require low-level integration of handwritten kernels. Instead, it leverages the highly optimized accurate kernel implementations maintained by the framework and therefore adds very little runtime overhead to the training procedure. Secondly, instead of selecting instances with unique characteristics out of a discrete (and potentially large) set of AMs, the AGN model captures their most relevant property—the non-recoverable error—in a single, continuous parameter. Only after solving the optimization problem in the more favorable AGN space, the found error robustness is used to select matching hardware instances.

3.2 Gradient-based Robustness Optimization

Every layer in our network has a perturbation factor σ_l which determines the amount of noise that is added to its accurate output. For each batch, the amount of perturbation is scaled by the standard deviation of the batch as proposed by Marchisio et al. [21]. The relative scaling avoids a situation where the effect of noise of a fixed magnitude would be diminished during training through the network optimizing towards greater pre-activation outputs [8]. To perturb the accurate calculation $\tilde{y}_l \in \mathbb{R}^m$ of a layer l , a tensor with random values of the same dimensions $\tilde{q} \sim \mathcal{N}_m(0, 1)$ is drawn from a normal distribution with a mean of zero and a standard deviation of one. The standard deviation still needs to be adjusted to match the standard deviation of the current batch; to achieve this relative scaling, the tensor is multiplied with the standard deviation of the accurate computation's output for the current batch $\sigma(\tilde{y}_l)$ and then weighted with the layer's perturbation factor σ_l before being added to the result of the accurate computation as shown in Figure 1.

$$\tilde{\tilde{y}}_l = \tilde{y}_l + \sigma_l \cdot \sigma(\tilde{y}_l) \cdot \tilde{q} \quad (7)$$

In the context of this model, the task loss \mathcal{L}_T can be differentiated directly w.r.t σ_l using the chain rule:

$$\frac{\partial \mathcal{L}_T}{\partial \sigma_l} = \frac{\partial \mathcal{L}_T}{\partial \tilde{\tilde{y}}_l} \cdot \frac{\partial \tilde{\tilde{y}}_l}{\partial \sigma_l} \quad (8)$$

$$= \frac{\partial \mathcal{L}_T}{\partial \tilde{\tilde{y}}_l} \cdot \sigma(\tilde{y}_l) \cdot \tilde{q} \quad (9)$$

Because this formulation is continuous and differentiable, it is possible to optimize all layer perturbations simultaneously—just like all other network parameters—using backpropagation. Computation errors in an early layer can impact the overall accuracy disproportionately as they might alter the results in all subsequent layers; these complex dynamics of propagating errors are already captured by this model because of the chained computation of gradients. The loss function is evaluated based on layers being perturbed by a certain amount of AGN, resulting in model convergence towards higher robustness to small perturbations. Through the added noise, the output of each individual neuron will be less reliable. Information relevant to the model's task will therefore have to be spread out over more neurons when propagating through the network, similar to the popular Dropout regularization [30]. We assume that this increased robustness will also be beneficial when deploying AMs: because the model has learned to be less reliant on the precise output of individual neurons, it will be able to handle slight deviations in the intermediate results caused by AMs better.

Only using the task loss to drive model optimization is not sufficient, however, since σ_l could always be driven towards zero. To avoid this, we introduce an additional noise loss \mathcal{L}_N that incentivizes the optimizer to explore solutions with higher perturbation. The noise loss takes into account the current values of σ_l as well as the relative cost of each layer $c_l = c(l) / \sum_{l \in L} c(l)$. The relative cost scales the importance of the amount of perturbation in each layer; it is clear that we care most about high values of σ_l in layers with a high complexity, while it is preferable to allow for higher relative accuracy in layers that do not contribute much to overall resource consumption. We choose the amount of multiplications in a layer as an easy to implement cost function $c(l)$. The additional noise loss solves the problem of the optimizer converging to solutions with no AGN, but it creates a new one: The optimizer could now decrease the total loss indefinitely by adding ever-growing amounts of noise to the intermediate results, making the task loss insignificant. We avoid this by upper-bounding the maximum allowable noise loss to some fixed value σ_{\max} . This gives us the total noise loss as

$$\mathcal{L}_N = - \sum_{l \in L} \min \{ |\sigma_l|, \sigma_{\max} \} \cdot c_l \quad (10)$$

The overall loss \mathcal{L} is then simply the weighted sum of task and noise loss

$$\mathcal{L} = \mathcal{L}_T + \lambda \cdot \mathcal{L}_N \quad (11)$$

where λ is a hyperparameter that determines the relative importance of network accuracy and perturbation. Equation (10) can be differentiated w.r.t. σ_l as

$$\frac{\partial \mathcal{L}_N}{\partial \sigma_l} = \begin{cases} -c_l, & |\sigma_l| \leq \sigma_{\max} \\ 0, & \text{otherwise} \end{cases} \quad (12)$$

After optimizing the amount of injected noise per layer we arrive at a configuration where each layer’s learned robustness to noise σ_l has been tuned to maximize the amount of overall AGN throughout the network while minimizing the degradation of accuracy. Each layer’s σ_l can be considered a proxy for the actual (but much harder) optimization task: determining how sensitive the network’s overall performance is to inaccurate computation results in each layer

3.3 Probabilistic Multi-Distribution Error Model

An important question that arises is how the abstract optimization factor σ_l in the AGN model relates to the error produced by a given AM. In order to link both, we propose the use of a probabilistic model that treats each error as a random event with certain probabilities; instead of truthfully simulating the error function for each pair of input values, its output can be considered a discrete random variable $Z = e(x, w)$ that maps the outcome of randomly selecting x and w to the error produced by these operands. Determining the standard deviation of Z makes it comparable with the learned perturbation factor σ_l that simulates the non-recoverable portion of the approximation error in the AGN space. Assuming the commonly used 8-bit Integer multipliers, both x and w can take $2^8 = 256$ distinct values for their sample spaces Ω_x and Ω_w . In total, there are 256^2 possible combinations of input values in the joint sample space $\Omega_Z = \Omega_x \times \Omega_w$. For any multiplier of interest, we need to know the error (i.e. the difference between accurate and approximate output) for each of these input combinations, from hereon referred to as the multiplier’s *error map*. This is the only part of the method that requires at least a high-level model of the hardware to be simulated. If simulating the hardware is expensive, this can be done once and the resulting error map stored for later use.

Next, we need to consider that not all 256 values that x and w might take are equally likely to appear. The relative frequencies of values in the weights tensor and an input sample can be used to model their probability distributions $p_x(x)$ and $p_w(w)$. In practice, this means building a histogram with the count of each possible 8-bit Integer value for both tensors and normalizing it to one. The data-driven construction of operand probabilities means that no assumptions have to be made with regards to their underlying distribution. Given the error for each combination of values and their respective likelihoods, mean and standard deviation of the error can be estimated as

$$\mu_Z = \sum_{x \in \Omega_x} \sum_{w \in \Omega_w} p_x(x) \cdot p_w(w) \cdot e(x, w) \quad (13)$$

$$\sigma_Z^2 = \sum_{x \in \Omega_x} \sum_{w \in \Omega_w} p_x(x) \cdot p_w(w) \cdot (e(x, w) - \mu_Z)^2 \quad (14)$$

which describes the mean and standard deviation of the error for a single multiplication. From Equation (2), it is clear that the neuron output is the sum over n multiplications. n is the *fan-in* of the neuron, or more simply the number of incoming connections. For CNNs and most other common NN architectures the fan-in is identical for all neurons in a layer. Under the assumption that x and w are independent and identically distributed (an assumption that we will address in more detail in the next paragraph), we can apply

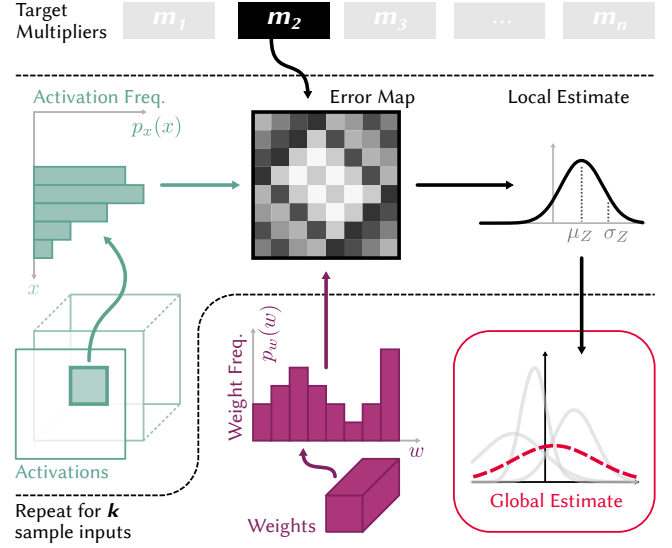


Figure 2: Process of deriving a global estimate of multiplier error properties from multiple local estimates.

the central limit theorem to the growth of the standard deviation. With this, the error mean at the neuron output scales linearly, while the standard deviation scales with the square root of the fan-in:

$$\begin{aligned} \mu_e &= n \cdot \mu_Z \\ \sigma_e &= \sqrt{n} \cdot \sigma_Z \end{aligned}$$

The second observation is important because it implies that layers with a higher fan-in will produce an error that is smaller relative to the magnitude of the output value (which grows with n), all other factors being equal.

So far, we have assumed x and w to be independent and identically distributed. Empirically validating this assumption shows that it holds well for weights, but not for activations. Intuitively, this can be explained by a higher amount of local correlations in the activations. To make this clearer, we can imagine a black and white image passing through a convolutional layer: because pixels of the same color tend to be grouped together, the individual patches are more likely to be all-black or all-white than the global distribution of pixels in the image would suggest. More concisely, the *local* distribution of feature values can deviate strongly from their *global* distribution.

The problem of diverging local and global distributions of operand values can be addressed through sampling; mean and standard deviation are first calculated for several samples of the local distribution. The sample is drawn from the receptive field of a neuron in the target layer, i.e. a sample is either a randomly selected input feature vector for Fully-Connected (FC) layers or a patch for convolutional layers. These individual observations are then integrated into an estimate of the global distribution’s mean and standard deviation as shown in Figure 2. We randomly sample k vectors from the layer’s input activations. For each input vector, a frequency distribution $p_x(x)$ is generated. Equations (13) and (14) are then used to calculate its mean and standard deviation. As an additional

benefit, this removes the need to build a global histogram of the input value distribution in favor of building multiple distributions on very small input samples. Calculating the combined mean of the local distributions is simple. Special care needs to be taken when combining group standard deviations: Our method must account for the effect of different means in each sample on the combined standard deviation [17].

$$\mu_Z = \frac{1}{k} \sum_{i=1}^k \mu_{Z_i} \quad (15)$$

$$\sigma_Z^2 = \frac{1}{k} \left[\sum_{i=1}^k (\sigma_{Z_i}^2 + \mu_{Z_i}^2) - \frac{1}{k} \left(\sum_{i=1}^k \mu_{Z_i} \right)^2 \right] \quad (16)$$

The degree with which this method is applicable is determined by the fan-in n of the respective layer, as convergence of the error towards a normal distribution depends primarily on the fan-in. If layers with a very low fan-in were present, some care would have to be taken to confirm that the AGN model is still valid.

3.4 Multiplier Matching

Our method focuses on Integer AMs with a low bit width which are typically used in low-energy inference settings like edge devices and accelerators. Because of the small amount of operand combinations, a full error map should normally be easy to obtain. To increase the degrees of freedom of the solution, having a large set of different AMs that cover a wide range of accuracy and resource consumption is desirable. As long as these conditions are met, our method is applicable to many different AMs designs.

With an optimized configuration of σ_l as a measure of a layer's sensitivity, we can match an appropriate AM to each layer. For every AM in our search space, we calculate an estimate of the error it produces using the method described in detail in Section 3.3. The estimate produced by the error model is directly comparable to the learned σ_l . The multipliers for which the error lies above the accuracy threshold σ_l are discarded since they do not produce the required accuracy. From the remaining set of multipliers that produce sufficiently accurate results, we can pick the one that optimizes another metric of interest.

4 RESULTS AND DISCUSSION

Unless stated otherwise, all experiments were carried out on a host system equipped with an AMD Ryzen 9 3900X CPU and a single nVidia RTX 2080Ti GPU. We implement our search algorithm [32] as an extension of the popular deep learning framework PyTorch [26].

4.1 Multi-Distribution Error Model

In order to assess the accuracy with which our error model can infer the standard deviation of the approximation error on the layer's output, we evaluate its performance on the layers of a ResNet8 model. The model is trained using the parameters laid out in Section 4.2. We do not explicitly evaluate the estimate of the error mean, as it is less relevant to our method for the reasons discussed in Section 3.1. From Equation (14), it should be clear that an accurate estimate of the error mean is a necessary condition for an

Table 1: Comparison of predictive methods for multiplier error standard deviation on ResNet8 layers

Error Model	Pearson Correlation	Median Relative Error ± Interquartile Range
Multiplier MRE [9]	0.546	n.a.
Single-Distribution MC [21]	0.767	(42.9 ± 53.2) %
Probabilistic Multi-Dist. (ours)	0.997	(4.6 ± 8.8) %

accurate estimate of the standard deviation. The ground truth for the approximation error is obtained through a behavioral simulation of all 13 unsigned multipliers from the EvoApprox library [23]. The simulation generates the approximated pre-activation output of each layer, given its weights and activations. We compare the measured error's standard deviation to the estimate of the standard deviation generated by our probabilistic multi-distribution error model for $k = 512$ input samples. The results are also compared to the single-distribution MC method discussed in [21]. We further include the respective multiplier's MRE in the evaluation as it is a commonly proposed [3, 9] single-value metric, used as an indication of multiplier performance. The results of our evaluation can be found in Table 1.

We find that the results of the Single-Distribution MC method are very similar to the results produced by using our probabilistic method *without* accounting for differing local distributions, i.e. based on the global frequency distribution of activation values alone. Single-Distribution MC and our probabilistic model converging to similar results in this scenario is very plausible, given that the former method is a MC simulation of exactly the same process that is analytically described in the latter. This suggests that taking local divergence of the input activations into account provides a significant boost in the predictive performance of our model, compared to methods that assume the global distribution to be present for all operations. The observed values for the standard deviation occupy a very wide numerical range of approximately 5 orders of magnitude. On such a large range, a median relative error of 4.6 % is negligible, which is reflected in the almost perfect correlation of 0.997.

Our evaluation shows that the predictive performance of the MRE for the error's standard deviation is very limited. This can be explained by the fact that the MRE is only a metric of a multiplier performance over the entire numerical range and for operands with equal probabilities. It does not distinguish between systematic and non-systematic portions of the error and can include neither knowledge about the different likelihoods of operands in NN models nor the impact of a layer's fan-in on the aggregate error at the layer output.

4.2 ResNet on CIFAR-10

In line with previous works [3, 25], our method is evaluated on several sizes of the ResNet [12] architecture, trained on the CIFAR-10 data set [15] with 36 8-bit unsigned multipliers from the EvoApprox library [23] as the AM search space. Relative power numbers were generated using the `pdk45_pwr` property of the EvoApprox multipliers, normalized to the power consumption of the reference accurate

Table 2: Comparison of energy reduction and accuracy loss for different methods

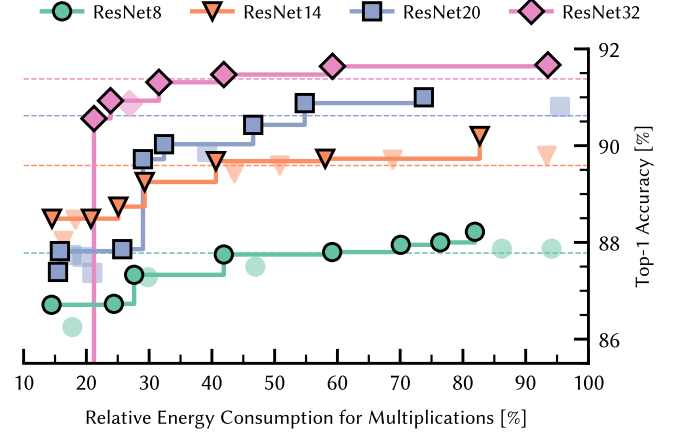
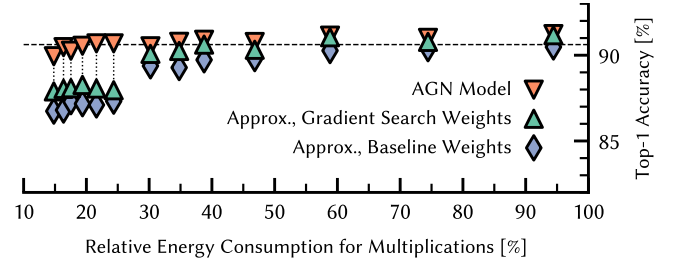
Model	Method	Energy Reduction	Top-1 Accuracy Loss [p.p.]
ResNet8	ALWANN [25]	30 %	1.7
	Uniform Retraining [3]	58 %	0.9
	Gradient Search (ours)	70 %	0.5
ResNet14	ALWANN [25]	30 %	0.9
	Uniform Retraining [3]	57 %	0.9
	Gradient Search (ours)	75 %	0.9
ResNet20	LVRM [31]	17 %	1.0
	Uniform Retraining [3]	53 %	0.7
	Gradient Search (ours)	71 %	0.9
ResNet32	Gradient Search (ours)	79 %	0.8

multiplier and weighted with the number of multiplications in each layer.

The training and augmentation procedure laid out in the original work is used to generate a floating-point reference model. Next, Quantization-aware Training (QAT) is carried out to obtain a baseline model that is quantized to 8 Bit. On the quantized baseline, we uniformly initialize each layer’s perturbation factor σ_l to 0.1 with a cap at $\sigma_{\max} = 0.5$. Layer perturbation factors and other network parameters are then jointly optimized for 30 epochs using the Stochastic Gradient Descent (SGD) optimizer with an initial learning rate of 1×10^{-2} and a decay of 0.9 after every 10 epochs. After matching AMs with appropriate accuracy to each layer, we retrain the entire network using behavioral simulation of the selected AMs for another 5 epochs with an initial learning rate of 1×10^{-3} and a decay of 0.9 after every other epoch. During this phase, the Straight-Through Estimator (STE) [1, 13] is used to derive valid gradients for the AMs. We repeat the Gradient Search and retraining several times while varying the λ parameter between 0 and 0.6 in steps of 0.05. By adjusting the value of λ , we can generate several solutions, each of which strikes a different balance between accuracy and perturbation (and thus, by extension, energy consumption).

In the comparison of results in Figure 3 it can be seen that the accuracy is above the baseline for all ResNet variants for an energy reduction of up to 45%. We attribute this to the perturbation acting as a form of learnable regularization; since all parameters are trained in the Gradient Search phase, the network converges towards a configuration that is both more resilient to approximation and generalizes better to unseen data. The drop in accuracy for higher degrees of approximation becomes increasingly steep for deeper models, most likely due to the accumulating effect of the approximation error.

The comparison of the accuracy in the AGN space (‘AGN Model’) with the accuracy that is achieved after retraining using behavioral simulation (‘Approx., Gradient Search Weights’) in Figure 4 reveals another interesting property: the accuracy of a retrained model under approximation is very similar to the accuracy exhibited by the model that is perturbed using AGN up to energy savings of around 60%. For more aggressive approximation, the relationship


Figure 3: Pareto Front and dominated points of energy and accuracy for different sizes of ResNet [12] on the CIFAR-10 data set [15]. Horizontal line marks 8-bit quantized baseline accuracy.

Figure 4: Comparison of perturbed accuracy and accuracy after retraining with weights and biases of AGN model and baseline model for ResNet20. Horizontal line marks 8-bit quantized baseline accuracy.

between both values deteriorates up to a gap of several percentage points. These models suffer from a significant degradation of accuracy under approximation, while the same is not true for the same model perturbed with comparable amounts of AGN. This can be interpreted as a shortcoming of the AGN model: AMs with very low energy consumption are more likely to produce localized error patterns which are insufficiently captured by the AGN model. The AGN model assumes an even spread of errors over all neurons. It is likely that a structured error has a more adverse effect on the propagation of information for some specific connections, widening the gap between predicted and achieved accuracy.

Figure 4 also provides some insight into the question of whether training in the AGN space has a positive carryover to model accuracy when deploying AMs. To make the impact of training with AGN on the achieved accuracy visible, we repeat the retraining using behavioral simulation based on the weights and biases of the baseline model (‘Approx., Baseline Weights’) instead of the weights and biases learned during the Gradient Search phase. We can see that the models trained using AGN consistently achieve

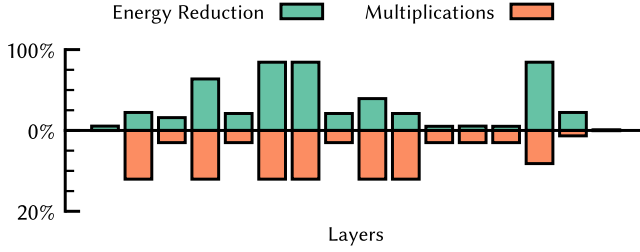


Figure 5: Comparison of energy reduction per layer and relative multiplications for VGG16, based on output configuration of unsigned EvoApprox multipliers

Table 3: Comparison of homogeneous and heterogeneous solutions for VGG16 [29] architecture on the Tiny ImageNet dataset [18]

Configuration	Energy Reduction	Top-5 Val. Accuracy
Baseline	n.a.	80.6 %
AGN Model, $\lambda = 0.3$	n.a.	80.2 %
Uniform Retraining, mul8s_1KVB	3.5 %	80.3 %
Heterogeneous, signed	11.6 %	80.5 %
Uniform Retraining, mul8u_19DB	52.7 %	79.6 %
Uniform Retraining, mul8u_185Q	52.7 %	79.7 %
Heterogeneous, unsigned	52.6 %	80.1 %

higher accuracies after retraining using behavioral simulation compared to models that directly attempt approximate retraining on the baseline model. This indicates that models trained using AGN have converged to a configuration that is more robust to the errors produced by approximation.

A comparison of the loss of accuracy and reduction in energy consumption to other state-of-the-art methods can be found in Table 2. In addition to improved energy efficiency, our algorithm adds little runtime overhead. The Gradient Search only takes between 6 min for ResNet8 and 16 min for ResNet32. Across all networks, this puts the overhead between 41 % to 45 % of the time taken to train the respective floating-point reference networks—much lower than the hours to days required by Mrazek et al. [25]. The multiplier matching algorithm that generates the estimated error standard deviation for each combination of layer and multiplier completes in around one minute for all surveyed networks on our target system.

4.3 VGG16 on Tiny ImageNet

To demonstrate the scalability of our method, we apply it to the more complex Tiny ImageNet dataset [18]. Tiny ImageNet is a smaller version of the ImageNet challenge [6] in which the number of classes is reduced from 1000 to 200. Each class contains 500 training and 50 validation images and images are down-scaled from 224×224 pixels to 64×64 pixels. The VGG16 CNN architecture [29] with additional batch normalization is used as a reference architecture. The SGD optimizer is used for all training runs as we find that the popular ADAM optimizer [14] does not produce

satisfactory results when optimizing the layer perturbations. Only a single run of Gradient Search with $\lambda = 0.3$ and an initial perturbation factor of $\sigma_l = 0.025$ for all layers is performed to account for the larger dataset. We also lower the amount of epochs for the Gradient Search and approximate retraining to 9 and 2 respectively. Based on the result in the AGN space, both the signed and unsigned 8-bit multipliers from the EvoApprox library are used separately as search spaces for matching AM instances.

Results in Table 3 show that heterogeneous configurations outperform uniform solutions when trading off energy savings and loss of accuracy. Given the more complex classification task, we do not find an improvement over the accuracy of the baseline model anymore, both in the AGN space as well as after deployment of AMs and retraining. The much lower reduction of energy consumption when using signed multipliers can be attributed their lower overall energy reduction for similar performance as well as the smaller search space of only 13 available signed 8-bit multipliers.

For the unsigned solution, the search procedure identifies 13 different AMs from the search space. The comparison of layer complexity and the respective reduction in energy consumption per layer in Figure 5 shows that the Gradient Search and subsequent multiplier assignment deploys the highest degrees of approximation on the network’s inner layers with high amounts of multiplications. In contrast, particularly the first and last layers are assigned highly accurate hardware instances. A relatively high sensitivity of these layers is in line with common heuristics in non-uniform quantization schemes [36].

We confirm that this effect is consistent by repeating the experiment with other CNN models. Performing the same optimization procedure on AlexNet [16] and MobileNetV2 [28] models yields similar results: Inner layers with higher computational complexity are assigned less accurate hardware instances with up to 84.4 % reduction in energy consumption. In contrast, highly accurate AMs with a reduction between 1.3 % and 5.4 % are mapped to the first and last layers of each model.

5 CONCLUSION

In this work, we have demonstrated the feasibility of combining heterogeneous approximation and retraining for NNs. The use of AGN as a surrogate model for behavioral simulation is motivated from the mathematical formulation of NNs. Our findings suggest that there is a strong connection between perturbation of neural networks with AGN and low to medium degrees of approximation. This connection, however, weakens for higher degrees of approximation. Whether the AGN model can be adapted to capture more structured errors without sacrificing generalizability remains to be answered by further research. Despite this, we show that the trade-off between energy and accuracy can be improved consistently and significantly by considering the varying robustness of different parts of a NN during the deployment of AMs. As a means to tackle the enormous search space of heterogeneous AM assignment, the flexibility of the AGN model is used to abstract over many different AMs with only a single parameter. This parameter is differentiable, so it can be learned using backpropagation. Learning the different degrees of robustness to errors during network training is the key to efficiently exploring different solutions, especially for deeper

networks. To connect AGN to concrete hardware, we introduced a probabilistic model of the approximation error. This model allows for an accurate prediction of the noise properties which the AM error will exhibit on any given layer without having to rely on time-consuming simulations. Through combining these methods, we provide a path towards NN hardware that makes inference both accurate and power-efficient.

REFERENCES

- [1] Yoshua Bengio, Nicholas Léonard, and Aaron C. Courville. 2013. Estimating or Propagating Gradients Through Stochastic Neurons for Conditional Computation. *CoRR* abs/1308.3432 (2013).
- [2] Nicholas Cheney, Martin Schrimpf, and Gabriel Kreiman. 2017. On the Robustness of Convolutional Neural Networks to Internal Architecture and Weight Perturbations. *CoRR* abs/1703.08245 (2017).
- [3] Cecilia De la Parra, Andre Guntoro, and Akash Kumar. 2020. Full Approximation of Deep Neural Networks through Efficient Optimization. In *IEEE International Symposium on Circuits and Systems, ISCAS 2020, Sevilla, Spain, October 10–21, 2020*.
- [4] Cecilia De la Parra, Andre Guntoro, and Akash Kumar. 2020. ProxSim: GPU-based Simulation Framework for Cross-Layer Approximate DNN Optimization. In *2020 Design, Automation & Test in Europe Conference & Exhibition, DATE 2020, Grenoble, France, March 9–13, 2020*.
- [5] Cecilia De la Parra, Andre Guntoro, and Akash Kumar. 2021. Efficient Accuracy Recovery in Approximate Neural Networks by Systematic Error Modelling. In *ASPDAC '21: 26th Asia and South Pacific Design Automation Conference, Tokyo, Japan, January 18–21, 2021*.
- [6] Jia Deng, Wei Dong, Richard Socher, Li-Jia Li, Kai Li, and Li Fei-Fei. 2009. ImageNet: A large-scale hierarchical image database. In *2009 IEEE Computer Society Conference on Computer Vision and Pattern Recognition (CVPR 2009), 20–25 June 2009, Miami, Florida, USA*.
- [7] Ahmed T. Elthakeb, Prannoy Pilligundla, Fatemehsadat Mireshghallah, Amir Yazdanbakhsh, and Hadi Esmailzadeh. 2020. ReLeQ : A Reinforcement Learning Approach for Automatic Deep Quantization of Neural Networks. *IEEE Micro* 40, 5 (2020), 37–45.
- [8] Ian J. Goodfellow, Yoshua Bengio, and Aaron C. Courville. 2016. *Deep Learning*. MIT Press.
- [9] Issam Hammad, Kamal El-Sankary, and Jason Gu. 2019. Deep Learning Training with Simulated Approximate Multipliers. In *2019 IEEE International Conference on Robotics and Biomimetics, ROBIO 2019, Dali, China, December 6–8, 2019*.
- [10] Song Han, Jeff Pool, John Tran, and William J. Dally. 2015. Learning both Weights and Connections for Efficient Neural Network. In *Advances in Neural Information Processing Systems 28: Annual Conference on Neural Information Processing Systems 2015, December 7–12, 2015, Montreal, Quebec, Canada*.
- [11] Muhammad Abdullah Hanif, Rehan Hafiz, and Muhammad Shafique. 2018. Error resilience analysis for systematically employing approximate computing in convolutional neural networks. In *2018 Design, Automation & Test in Europe Conference & Exhibition, DATE 2018, Dresden, Germany, March 19–23, 2018*.
- [12] Kaiming He, Xiangyu Zhang, Shaoqing Ren, and Jian Sun. 2016. Deep Residual Learning for Image Recognition. In *2016 IEEE Conference on Computer Vision and Pattern Recognition, CVPR 2016, Las Vegas, NV, USA, June 27–30, 2016*.
- [13] Xin He, Liu Ke, Wenyan Lu, Guihai Yan, and Xuan Zhang. 2018. AxTrain: Hardware-Oriented Neural Network Training for Approximate Inference. In *Proceedings of the International Symposium on Low Power Electronics and Design, ISLPED 2018, Seattle, WA, USA, July 23–25, 2018*.
- [14] Diederik P. Kingma and Jimmy Ba. 2015. Adam: A Method for Stochastic Optimization. In *3rd International Conference on Learning Representations, ICLR 2015, San Diego, CA, USA, May 7–9, 2015*.
- [15] Alex Krizhevsky, Geoffrey Hinton, et al. 2009. Learning multiple layers of features from tiny images. (2009).
- [16] Alex Krizhevsky, Ilya Sutskever, and Geoffrey E. Hinton. 2012. ImageNet Classification with Deep Convolutional Neural Networks. In *Advances in Neural Information Processing Systems 25: 26th Annual Conference on Neural Information Processing Systems*.
- [17] Ingo Lange. 2018. Standardabweichungen und Kovarianzen über mehrere Mittelungsintervalle. <https://wettermast.uni-hamburg.de/Downloads/StdAbwKovIntervalle.pdf>
- [18] Ya Le and Xuan S. Yang. 2015. Tiny ImageNet Visual Recognition Challenge.
- [19] Yuhang Li, Wei Wang, Haoli Bai, Ruihao Gong, Xin Dong, and Fengwei Yu. 2020. Efficient Bitwidth Search for Practical Mixed Precision Neural Network. *CoRR* abs/2003.07577 (2020).
- [20] Uros Lotric and Patricio Bulic. 2012. Applicability of approximate multipliers in hardware neural networks. *Neurocomputing* 96 (2012), 57–65.
- [21] Alberto Marchisio, Vojtech Mrazek, Muhammad Abdullah Hanif, and Muhammad Shafique. 2020. ReD-CaNe: A Systematic Methodology for Resilience Analysis and Design of Capsule Networks under Approximations. In *2020 Design, Automation & Test in Europe Conference & Exhibition, DATE 2020, Grenoble, France, March 9–13, 2020*.
- [22] Sana Mazahir, Osman Hasan, Rehan Hafiz, and Muhammad Shafique. 2017. Probabilistic Error Analysis of Approximate Recursive Multipliers. *IEEE Trans. Computers* 66, 11 (2017), 1982–1990.
- [23] Vojtech Mrazek, Radek Hrbacek, Zdenek Vasicek, and Lukás Sekanina. 2017. EvoApprox8b: Library of approximate adders and multipliers for circuit design and benchmarking of approximation methods. In *Design, Automation & Test in Europe Conference & Exhibition, DATE 2017, Lausanne, Switzerland, March 27–31,*

- 2017.
- [24] Vojtech Mrazek, Syed Shakib Sarwar, Lukás Sekanina, Zdenek Vasicek, and Kaushik Roy. 2016. Design of power-efficient approximate multipliers for approximate artificial neural networks. In *Proceedings of the 35th International Conference on Computer-Aided Design, ICCAD 2016, Austin, TX, USA, November 7–10, 2016*.
 - [25] Vojtech Mrazek, Zdenek Vasicek, Lukás Sekanina, Muhammad Abdullah Hanif, and Muhammad Shafique. 2019. ALWANN: Automatic Layer-Wise Approximation of Deep Neural Network Accelerators without Retraining. In *Proceedings of the International Conference on Computer-Aided Design, ICCAD 2019, Westminster, CO, USA, November 4–7, 2019*.
 - [26] Adam Paszke, Sam Gross, Francisco Massa, Adam Lerer, James Bradbury, Gregory Chanan, Trevor Killeen, Zeming Lin, Natalia Gimelshein, Luca Antiga, Alban Desmaison, Andreas Köpf, Edward Z. Yang, Zach DeVito, Martin Raison, Alykhan Tejani, Sasank Chilamkurthy, Benoit Steiner, Lu Fang, Junjie Bai, and Soumith Chintala. 2019. PyTorch: An Imperative Style, High-Performance Deep Learning Library. *CoRR* abs/1912.01703 (2019).
 - [27] Michal Pinos, Vojtech Mrazek, and Lukás Sekanina. 2021. Evolutionary Neural Architecture Search Supporting Approximate Multipliers. In *Genetic Programming - 24th European Conference, EuroGP 2021, Virtual Event, April 7–9, 2021*.
 - [28] Mark Sandler, Andrew G. Howard, Menglong Zhu, Andrey Zhmoginov, and Liang-Chieh Chen. 2018. MobileNetV2: Inverted Residuals and Linear Bottlenecks. In *2018 IEEE Conference on Computer Vision and Pattern Recognition, CVPR 2018, Salt Lake City, UT, USA, June 18–22, 2018*.
 - [29] Karen Simonyan and Andrew Zisserman. 2015. Very Deep Convolutional Networks for Large-Scale Image Recognition. In *3rd International Conference on Learning Representations, ICLR 2015, San Diego, CA, USA, May 7–9, 2015*.
 - [30] Nitish Srivastava, Geoffrey Hinton, Alex Krizhevsky, Ilya Sutskever, and Ruslan Salakhutdinov. 2014. Dropout: a simple way to prevent neural networks from overfitting. *The journal of machine learning research* 15, 1 (2014), 1929–1958.
 - [31] Zois-Gerasimos Tasoulas, Georgios Zervakis, Iraklis Anagnostopoulos, Hussam Amrouch, and Jörg Henkel. 2020. Weight-Oriented Approximation for Energy-Efficient Neural Network Inference Accelerators. *IEEE Trans. Circuits Syst.* (2020).
 - [32] Elias Trommer. 2022. agn-approx Software Repository. <https://github.com/etrommer/agn-approx>. *GitHub repository* (2022).
 - [33] Elias Trommer, Bernd Waschneck, and Akash Kumar. 2021. dCSR: A Memory-Efficient Sparse Matrix Representation for Parallel Neural Network Inference. In *IEEE/ACM International Conference On Computer Aided Design, ICCAD 2021, Munich, Germany, November 1–4, 2021*.
 - [34] Salim Ullah, Siva Satyendra Sahoo, and Akash Kumar. 2021. CLAppED: A Design Framework for Implementing Cross-Layer Approximation in FPGA-based Embedded Systems. In *58th ACM/IEEE Design Automation Conference, DAC 2021, San Francisco, CA, USA, December 5–9, 2021*.
 - [35] Filip Vaverka, Vojtech Mrazek, Zdenek Vasicek, and Lukás Sekanina. 2020. TFApprox: Towards a Fast Emulation of DNN Approximate Hardware Accelerators on GPU. In *2020 Design, Automation & Test in Europe Conference & Exhibition, DATE 2020, Grenoble, France, March 9–13, 2020*.
 - [36] Kuan Wang, Zhijian Liu, Yujun Lin, Ji Lin, and Song Han. 2019. HAQ: Hardware-Aware Automated Quantization With Mixed Precision. In *IEEE Conference on Computer Vision and Pattern Recognition, CVPR 2019, Long Beach, CA, USA, June 16–20, 2019*.
 - [37] Xiaowei Xu, Yukun Ding, Sharon Xiaobo Hu, Michael Niemier, Jason Cong, Yu Hu, and Yiyu Shi. 2018. Scaling for edge inference of deep neural networks. *Nature Electronics* 1, 4 (2018), 216–222.
 - [38] Kohei Yamamoto. 2021. Learnable Companding Quantization for Accurate Low-Bit Neural Networks. In *IEEE Conference on Computer Vision and Pattern Recognition, CVPR 2021, virtual, June 19–25, 2021*.
 - [39] Dongqing Zhang, Jiaolong Yang, Dongqiangzi Ye, and Gang Hua. 2018. LQ-Nets: Learned Quantization for Highly Accurate and Compact Deep Neural Networks. In *Computer Vision - ECCV 2018 - 15th European Conference, Munich, Germany, September 8–14, 2018, Proceedings, Part VIII*.
 - [40] Qian Zhang, Ting Wang, Ye Tian, Feng Yuan, and Qiang Xu. 2015. ApproxANN: an approximate computing framework for artificial neural network. In *Proceedings of the 2015 Design, Automation & Test in Europe Conference & Exhibition, DATE 2015, Grenoble, France, March 9–13, 2015*.
 - [41] Ritchie Zhao, Yuwei Hu, Jordan Dotzel, Christopher De Sa, and Zhiru Zhang. 2019. Improving Neural Network Quantization without Retraining using Outlier Channel Splitting. In *Proceedings of the 36th International Conference on Machine Learning, ICML 2019, 9–15 June 2019, Long Beach, California, USA*.